Details of the beam plasma system and reproduction of ITER relevant EP simulations

Nakia Carlevaro[1,2], Giovanni Montani[1,3], Fulvio Zonca[1]

[1]ENEA, FSN Dept., C.R. Frascati, Via E. Fermi 45, 00044 Frascati, Italy.
[2]LTCalcoli Srl, Via Bergamo 60, 23807 Merate (LC), Italy.
[3]Physics Dept., "Sapienza" University of Rome, P.le Aldo Moro 5, 00185 Roma, Italy.

NAT VC, 19th July 2018

Hamiltonian description of beam-plasma systems

Beam-plasma system (BPS): fast **electron beam** injected into a **1D plasma**, treated as a **cold** linear dielectric medium ($\boldsymbol{\epsilon = 1 - \omega_p^2/\omega_j^2 \simeq 0}$) supporting longitudinal electrostatic **Langmuir waves** (m modes at the plasma frequency ω_p). Tenuous beam: $\eta \equiv n_B/n_p \ll 1$ (beam density n_B and plasma density n_p). Evolutive equations:

$$\bar{x}_i' = u_i\ , \qquad u_i' = \sum_{j=1}^{m} \left(i\,\ell_j\,\bar{\phi}_j\,e^{i\ell_j\bar{x}_i} + c.c. \right)\ , \tag{1a}$$

$$\bar{\phi}_j' = -i\bar{\phi}_j + \frac{i\eta}{2\ell_j^2 N}\sum_{i=1}^{N} e^{-i\ell_j\bar{x}_i}\ . \tag{1b}$$

Notation: 1D cold plasma equilibrium taken as a periodic slab of length L; particle positions along the x direction labeled by x_i, with $i = 1, \ldots N$ (N being the total particle number), and scaled as $\bar{x}_i = x_i(2\pi/L)$; Langmuir scalar potential $\varphi(x, t)$ expressed with Fourier components $\varphi_j(k_j, t)$; $\tau = t\omega_p$ and $(\ldots)' = \partial_\tau(\ldots)$, $\phi_j = (2\pi/L)^2 e\varphi_j/m\omega_p^2$, $\ell_j = k_j(2\pi/L)^{-1}$, $u_i = \bar{x}_i' = v_i(2\pi/L)/\omega_p$, $\bar{\phi}_j = \phi_j e^{-i\tau}$; frequencies/growth-rates normalized as $\bar{\omega} = \omega/\omega_p$, $\bar{\gamma} = \gamma/\omega_p$. Positions $\bar{x}_i$ ($N \simeq 10^6$) are initialized uniformly in $[0,\ 2\pi]$, while modes at $\mathcal{O}(10^{-14})$ to ensure initial linear response.

- Resonant mode (**linearly unstable**): $\ell_j u_{rj} = 1$ (phase vel. = beam vel.).

Non-linear features of beam-plasma systems

Dynamics of **one isolated wave**: exponential growth of the mode followed by non-linear saturation ($|\bar{\phi}|^S$). Particles get trapped in the potential well: phase-space rotating clumps.

- **Quadratic scaling**: $|\bar{\phi}|^S = \beta\bar{\gamma}_L^2$ with $\beta = const.$

- **Trapping (bounce) frequency**: $\bar{\omega}_B = \sqrt{2\ell^2|\bar{\phi}|^S} = \sqrt{2\beta}\ell\bar{\gamma}_L$ (approx. post-saturation motion as instantaneous harmonic oscillator).

- **Clump width** Δu^c_{NL}: measure the largest velocity of particles initialized with $u < u_r$ and the smallest velocity of particles with $u > u_r$. Measure during the temporal evolution: Δu^c_{NL} is taken as the value at saturation time τ_S and **analyzed vs. linear growth rate**.

- **Initial conditions** - Warm beam (particle number) distribution function in velocity $F_0(u) = 0.5\ \mathrm{Erfc}[a - b\, u]$ ($a \simeq 6.8$, $b \simeq 4537$).

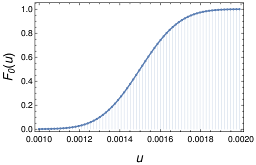

- **Reference case -** $u_r = 0.0015$ (inflection), $\eta \in [0.00015, 0.0025]$:

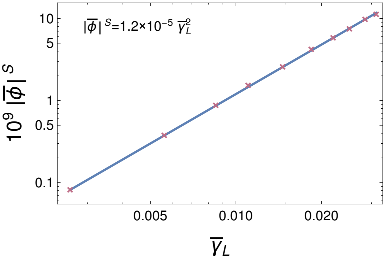

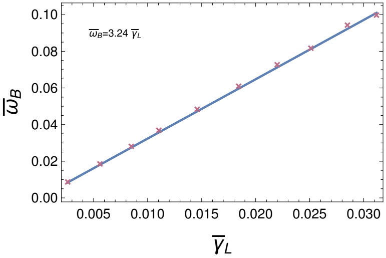

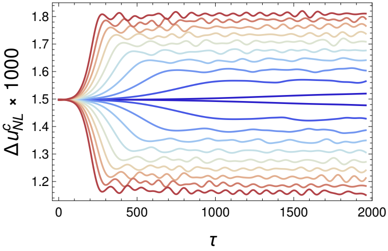

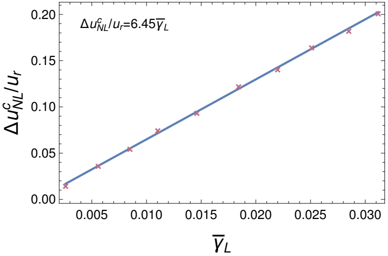

- **Global dependences** - Analysis of 5 distinct cases having equispaced resonant velocities in [0.0013, 0.0017].

  - For each case, 10 simulations by varying η in [0.00015, 0.0025] are studied (giving distinct drives $\bar{\gamma}_L$).

  - Averaged behaviors (consistent with existing literature):

$$\bar{\omega}_B = (3.31 \pm 0.06)\, \bar{\gamma}_L \; , \tag{2}$$

$$\Delta u^c_{NL}/u_r = (6.64 \pm 0.12)\, \bar{\gamma}_L \; . \tag{3}$$

  cf. [Y. Wu et al., *Phys. Plasmas* **2**, 4555 (1995)]
  cf. [L. Chen, F.Zonca, *Rev. Mod. Phys.* **88**, 015008 (2016)]

- **Note** - These behaviors are intrinsically dependent on initial conditions: the chosen distribution function mimics standard (slowing-down) **EP profile** in real systems.

Characterization of resonance overlap

System of three modes: study of resonance overlap at **saturation time**.

- Analyzed case: $u_{r1} \simeq 0.0013$, $u_{r2} \simeq 0.0015$, $u_{r3} = 0.0017$.
Onset of the overlap regime for $\eta \geqslant 0.00055$. Mode evolution:

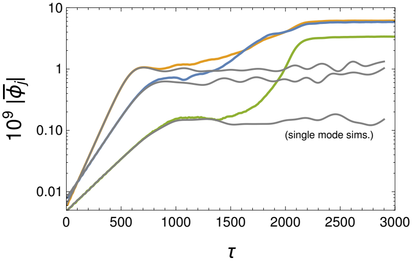

- This is due to the to the progressive **enhancement of the non-linear velocity spread**.
- **Note** - The present analysis focus on saturation time: different estimates could be obtained for later evolution.

Resonance overlap is assumed when **phase-space regions mix**.
Resonances and Δu^c_{NL} (dashed lines) for the threshold value $\eta = 0.00055$:

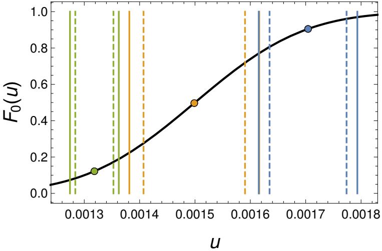

Non-linear trapping regions appear non-overlapped: **scale factor** applied to Δu^c_{NL}, to obtain overlap at saturation time (solid lines):

$$\Delta u_{NL} \simeq \alpha \Delta u^c_{NL} \;, \qquad \alpha \simeq 1.28 \;. \tag{4}$$

- **Transition to stochasticity** $\rightarrow$ Chirikov criterion: **self-consistently** determined (perturbation usually externally imposed).

Details in [F. Zonca, *IFTS Intensive Course on Advanced Plasma Physics*, Lecture 6, Spring 2011]
cf. [D.F. Escande, F. Doveil, *J. Stat. Phys.* **26**, 257 (1981)]
cf. [A.J. Lichtenberg, M.A. Lieberman, *Regular and Chaotic Dynamics - Second Edition* (Springer-Verlag) (2010)]

- Resonance u_{r1} (green) is initially isolated: the **synergistic non-linear interaction** of the two overlapping resonances (**non-linearly amplified**) modifies the dynamics and **broadens** the effective non-linear velocity spread (overlap with u_{r1} at later times).

- **Dynamic role of un-trapped particles.** Example of the function f_B evolved at saturation in the presence of only the resonance u_{r2}:

$$\Delta u^c_{NL}/u_r \simeq 6.64\,\bar{\gamma}_L \quad \text{(dashed)},$$
$$\Delta u_{NL}/u_r \simeq 8.5\,\bar{\gamma}_L \quad \text{(solid)}.$$

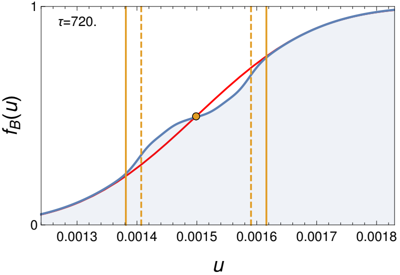

Only the effective Δu_{NL} well **characterizes the global distortion** of $f_B(\tau_S)$ **at stauration** from F_0 (red).

- Un-trapped particles are relevant in the **active overlap**: **power transfer** also involves particles simultaneously feeling multiple modes.

  cf. [L. Chen, F.Zonca, *Rev. Mod. Phys.* **88**, 015008 (2016)]

  cf. [D.F. Escande et al., *Rev. Mod. Plasma Phys.* (to be published).]

- **FTLE analysis** - Definition of **transport barriers** at saturation time $\tau = \tau_S = 700$. Same example of u_{r2} (Δu^c_{NL} dashed, Δu_{NL} solid). Short evolution - clump width:

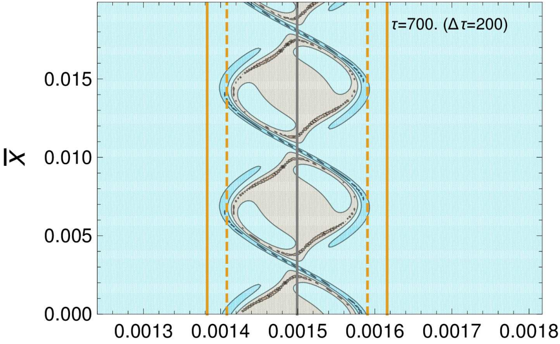

Very preliminary results (!)

[Collaboration with **M. Falessi**]

- Un-trapped particles are relevant in the **active overlap**: **power transfer** also involves particles simultaneously feeling multiple modes.
  cf. [L. Chen, F.Zonca, *Rev. Mod. Phys.* **88**, 015008 (2016)]
  cf. [D.F. Escande et al., *Rev. Mod. Plasma Phys.* (to be published).]
- **FTLE analysis** - Definition of **transport barriers** at saturation time $\tau = \tau_S = 700$. Same example of u_{r2} (Δu^c_{NL} dashed, Δu_{NL} solid). Late evolution - effective region of non-vanishing power transfer (?):

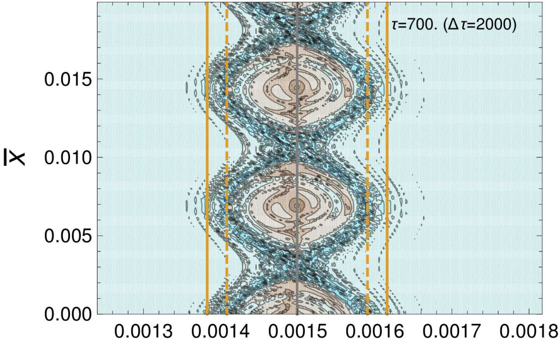

Very preliminary results (!)
[Collaboration with **M. Falessi**]

- **FTLE for multiple resonances** - Self-consistent evolution of the 3-mode system $u_{r1,2,3}$: $\tau = 400$

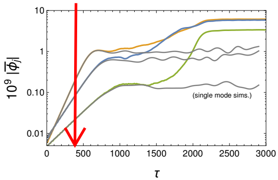

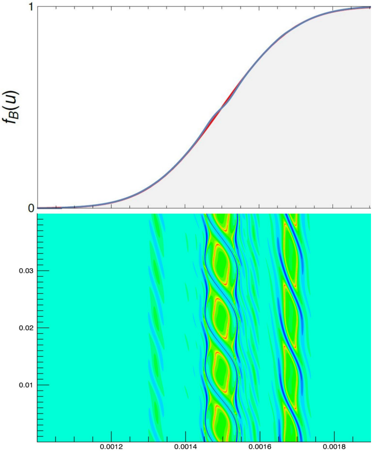

- Rich dynamics, presence of secondary resonances.

[Data analysis: G. Di Giannatale]

- **FTLE for multiple resonances** - Self-consistent evolution of the 3-mode system $u_{r1,2,3}$: $\tau = 1500$

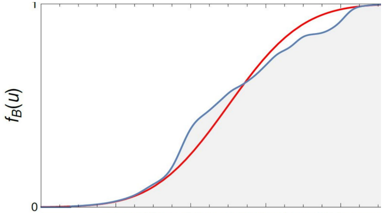

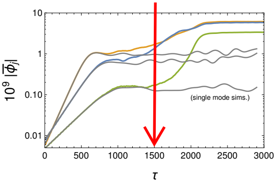

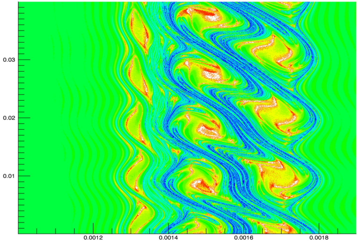

- Rich dynamics, presence of secondary resonances.

[Data analysis: G. Di Giannatale]

- **FTLE for multiple resonances** - Self-consistent evolution of the 3-mode system $u_{r1,2,3}$: $\tau = 1900$

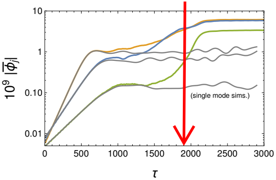

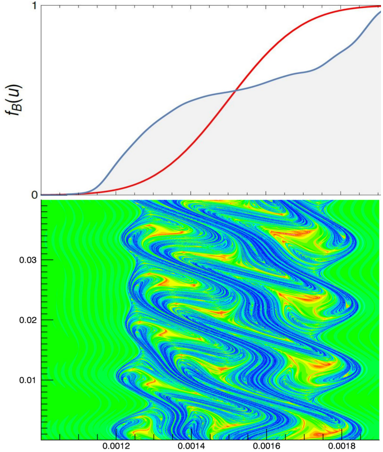

- Rich dynamics, presence of secondary resonances.

[Data analysis: G. Di Giannatale]

Mapping procedure [Collaboration with Ph. Lauber and T. Hayward]

Description of the mapping technique between the reduced **radial profile** r for the EP interacting with the Alfvénic spectrum and the **BPS velocity** space. One-to-one link formally derived from the resonance condition.

- **Single resonance** - Using two suitable normalization constants $\Omega_{1,2}$:

$$\frac{\omega_r^{AE}(r) - \omega_r^{AE}(r_r)}{\Omega_1} = \frac{k_r(v - v_r)}{\Omega_2} \; . \tag{5}$$

Notation: ω^{AE} is the mode frequency in the EP/AE framework. The normalized Tokamak radius is $s = r/a$ (a minor radius). For frequencies (growth rates and damping) we use $\bar{\omega}^{AE} = \omega^{AE}/\Omega_1$ ($\bar{\gamma}^{AE} = \gamma^{AE}/\Omega_1$) with $\Omega_1 = \omega_{A0}$ ($\omega_{A0} = v_{A0}/R_0$). Furthermore n^{AE} will denote the toroidal mode number.

- **Local map** trough the expansion $\bar{\omega}_r^{AE}(s) = \bar{\omega}_r^{AE}(s_r) + (s - s_r)\partial_s\bar{\omega}_r^{AE}$:

$$v = v_r - \frac{|\Omega_2 \partial_s \bar{\omega}_r^{AE}|}{k_r}(s - s_r) \; . \tag{6}$$

Imposing boundary and resonance conditions:

$$\boldsymbol{u = (1 - s)/\ell_1} \; , \tag{7}$$

ℓ_1 is arbitrarily fixed (spectral features and periodicity length).

- **Drive definition** - BPS closed by fixing η. EP/AE system has an higher dimensionality (3D): the radial profile emerges as an average procedure. **Non-linear transport in the BPS is more efficient**: linear growth rates normalized to the mode frequency are imposed

$$\frac{\bar{\gamma}_L}{\bar{\omega}_0} = \alpha\,\frac{\bar{\gamma}_L^{AE}}{\bar{\omega}^{AE}}\;, \quad \text{with } \alpha \leqslant 1\,. \tag{8}$$

  η is determined by the dispersion relation with EP radial profile $F_{H0}(s) \to F_{B0}(u)$. **3D-model** under construction.

- **Multiple modes** - The drive parameter can be fixed for one single reference resonance: **first intrinsic discrepancy**. The whole spectrum is addressed by means of the proper resonance conditions:

$$\ell_{r(j)} = \ell_1/(1 - s_{r(j)})\,. \tag{9}$$

- **Damping** - Preserve the asymptotic mode decay:

$$\bar{\gamma}_{d(j)}/\bar{\omega}_{0(j)} = \bar{\gamma}_{d(j)}^{AE}/\bar{\omega}_j^{AE}\,. \tag{10}$$

Numerical results

Study of the reduced ITER 15MA beseline scenario in SLB16:
[M. Schneller, Ph. Lauber, S. Briguglio, *Plasma Phys. Control. Fusion* **58**, 014019 (2016)]

- **Parameter setup and linear analysis** - Initial EP slowing down:

$$F_{H0}(s) = 0.5\,\mathrm{Erfc}[-1.2 + 3.2s]\,. \tag{11}$$

Least damped **27 TAE**: $n^{AE} \in [12, 30]$ for the main branch (red) and $n^{AE} \in [5, 12]$ for the low branch (blue).

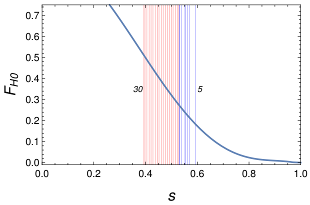

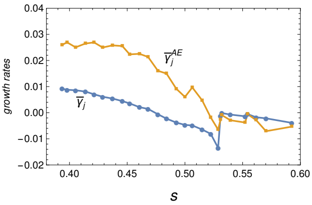

Reference resonance: $n^{AE} = 21$. **Optimization for $\alpha = 0.4$.**

- Growth rate profile reliable for the main branch. **Discrepancy** for the low branch: TAE freq. change significantly and this is not accounted in BPS.

- **Mode evolution** - Comparison of the multi mode simulations (bright colors) with respect to the 27 runs of single mode (opaque colors).

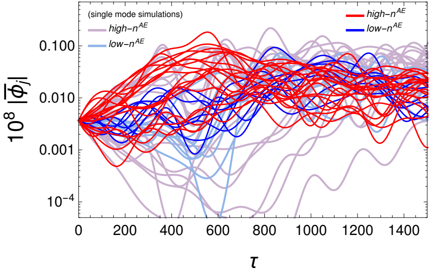

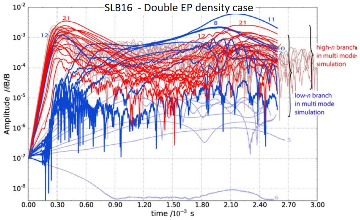

- low-n^{AE} branch (blue) is more efficiently and rapidly excited in the simultaneous presence of the modes (despite the negative drive) due to the expected **avalanche transport**.

- As in SLB16, the saturation level of some modes is larger than the corresponding single mode evolution (less evident due the scaling).

- **EP redistribution** - Spectral evolution reflects on the EP profile:

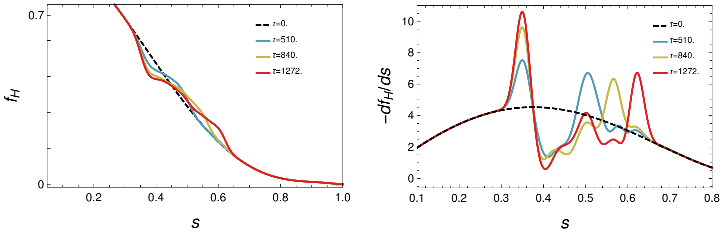

- **Convective transport** toward the plasma edge.

- A second peak (low branch) is shifting in time toward $s \simeq 6.5$.

- Fixed set of modes: the transport process is **bounded** due to the absence of further unstable modes.

- In SLB16, outer redistribution triggered toward $s \simeq 0.85$: importance of the **poloidal harmonics** spectrum.

- **EP redistribution** - Spectral evolution reflects on the EP profile:

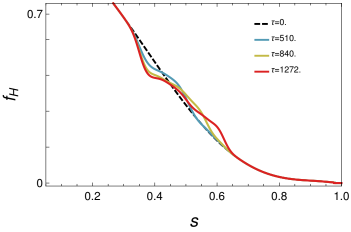

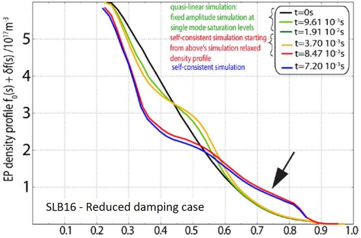

- **Convective transport** toward the plasma edge.

- A second peak (low branch) is shifting in time toward $s \simeq 6.5$.

- Fixed set of modes: the transport process is **bounded** due to the absence of further unstable modes.

- In SLB16, outer redistribution triggered toward $s \simeq 0.85$: importance of the **poloidal harmonics** spectrum (low branch has been simulated with 12 poloidal harmonics, the high branch with 2).

- **Comparison with QL transport** - QL equations r-dimension:

[N. Carlevaro, A.V. Milovanov, M.V. Falessi, G. Montani, D. Terzani and F. Zonca, Entropy 18, 143 (2016)]

$$f_H = F_{H0} - \pi \bar{\mathcal{N}} R \partial_s [(1-s)^{-5} \bar{\mathcal{I}}] \,, \tag{12a}$$

$$\partial_t \bar{\mathcal{I}} = -\frac{\eta}{R}(1-s)^2\, \bar{\mathcal{I}}\, \partial_s F_{H0} + \pi\eta(1-s)^2 \bar{\mathcal{N}}\, \bar{\mathcal{I}}\, \partial_s^2 [(1-s)^{-5} \bar{\mathcal{I}}] \,. \tag{12b}$$

Notation: $R = \int_{-\infty}^{+\infty} ds F_{H0}$, while the spectrum is $\bar{\mathcal{I}}(\tau, s) = \ell_1^5 |\bar{\phi}|^2/\eta$. $\bar{\phi}(\tau, s)$ is the continuous mode spectrum derived from the discrete one, specified by means of the resonance conditions. $\bar{\mathcal{N}} = m/\Delta\ell$ is spectral density and $\Delta\ell = \mathrm{Max}[\ell] - \mathrm{Min}[\ell]$ the spectral width.

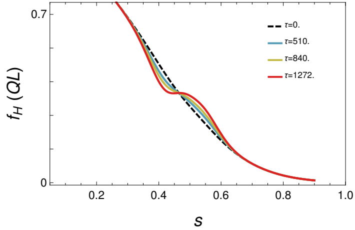

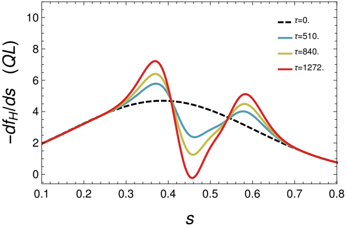

- Absence of avalanche: two well **localized peaks** avoiding the outer redistribution. QL model not predictive.

- **The role of harmonics** - Model with other 20 modes having wave numbers resonating with $0.55 \leqslant s \leqslant 0.95$. Given the linear setup (thus $\bar{\gamma}_{L(h)}$), specific damping rates $\bar{\gamma}_{d(h)}$ are introduced to get a **Gaussian distribution for the drive** $\bar{\gamma}_{(h)} = \bar{\gamma}_{L(h)} - \bar{\gamma}_{d(h)}$:

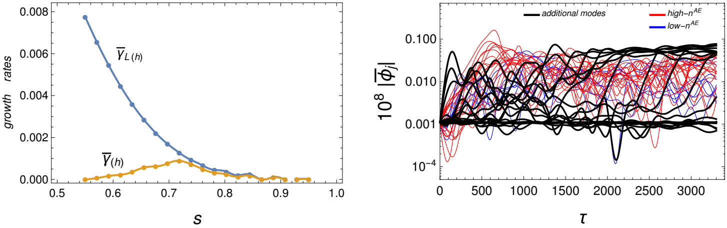

- Mode evolution: **spectral transfer** clearly emerges.
Additional modes progressively excited.

Increased **avalanche transport** toward large radial positions.
Outer redistribution is triggered around $s \simeq 0.75$:

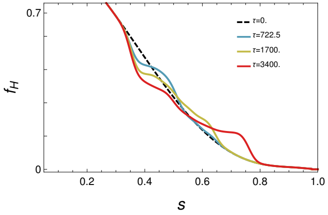

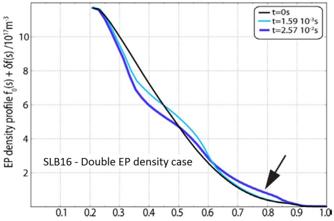

- Domino effects is **less efficient** in the BPS due to the fixed character of the spectrum which can not mimic in the very details the harmonics effects near the edge.

- Despite the differences, the **non-pure diffusive** character of the transport is enlightened.

Summary of the results

- Characterization of **resonance overlap** and proper definition of the **non-linear velocity spread** in the BPS:
  - the fully self-consistent analysis agrees qualitatively and quantitatively with existing studies of the transition to the stochasticity made by dynamical system theory.
- **Mapping procedure** between the velocity space of the BPS and the radial configurations concerning the transport properties of fast ions interacting with TAE in a Tokamak device:
  - clear evidence of avalanche processes and convective transport toward the plasma edge;
  - despite the successes of the mapping predictions, at the present level, the agreement with the Hagis-Ligka simulations still remains on a qualitative level;
  - strongly limited by the difference existing in the phenomenology of the two systems and therefore it require a very detailed calibration.

Backup slides: FTLE

Sensitive dependence of trajectories on initial conditions
$\rightarrow$ **Finite Time Lyapunov Exponents** (FTLE)

- *measure of the degree of instability*.

Single trajectory: $\mathbf{x}(\tau)$
Nearby trajectory: $\mathbf{x}'(\tau) \rightarrow \mathbf{x}'(\tau_0) = \mathbf{x}(\tau_0) + \delta(\tau_0)$

- Non-chaotic systems: $\delta(\tau)$ remains bounded.
- Chaotic systems: $\delta(\tau) \sim \delta(\tau_0)\, e^{\gamma\tau}$ γ: local rate of expansion.

Non-fluctuating par. characterizing instability: **maximum** FTLE

$$\lambda_{max} = \frac{\ln(\delta(\tau^*)/\delta(0))}{\tau^* - \tau_0} \qquad \Delta\tau = \tau^* - \tau_0$$

Find **transport barriers**

1. Extract time evolution of the potentials ϕ from simulations.
2. Use it to explore the whole phase-space trajectories by monitoring a **two grids** (having an initial displacement $\delta\tau_0$) of different initial conditions.

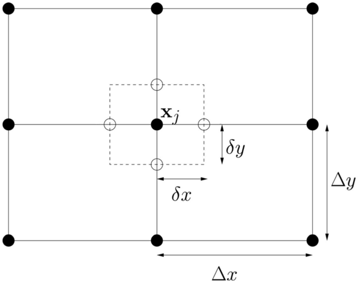

Ongoing - Vlasov-Poisson system: 3 different approaches

Vlasov-Poisson coupled system for the BPS:

$$\partial_t E_k = -i\omega_p E_k + \frac{2\pi e\omega_p}{k}\int_{-\infty}^{\infty} dv f_k \;, \quad \partial_t f_k = -ikvf_k + \frac{e}{m}\sum_q E_{k-q}\partial_v f_q \;.$$

- $f_{k=0} \equiv \hat{f}_B$ is the only contribution having a non-zero initial condition (BPS initially homogeneous), *i.e.*, $f_{k=0}(t=0,v) \equiv \hat{F}_B(v)$:

$$\partial_t \hat{f}_B = \frac{e}{m}\sum_q E_{-q}\partial_v f_q \;.$$

- **Assumption**: f_k receives mainly contribution from $q = k$:

$$\partial_t f_k = -ikv\, f_k + \frac{e}{m}E_k \partial_v \hat{f}_B \;.$$

Substituting and using the complex-conjugate notation:

$$\partial_t \hat{f}_B(t,v) - \frac{e^2}{m^2}\sum_k \Big[E_k^*\,\partial_v\Big(\int_0^t dy E_k(y) e^{ikv(t-y)}\partial_v \hat{f}_B(y,v)\Big) + c.c.\Big] = 0 \;.$$

- **Dyson equation** - Fully self consistent scheme. Without loss of generality, the electric field can be set as

$$E_k(y) = E_k(t)\, \exp\Big[-i\int_t^y dx\omega_k(x)\Big]\,.$$

A Dyson like equation for $\hat{f}_B(t,v)$ can be obtained:

$$\begin{aligned}\partial_t \hat{f}_B(t,v) = \frac{e^2}{m^2}\sum_k |E_k(t)|^2 \times \\ \times\, \partial_v\Big[\int_0^t dy \exp\Big(ikv(y-t) - i\int_t^y dx\,\omega_k(x)\Big)\partial_v \hat{f}_B(y,v) + \\ + \int_0^t dy \exp\Big(-ikv(y-t) - i\int_t^y dx\,\omega_k^*(x)\Big)\partial_v \hat{f}_B(y,v)\Big]\,,\end{aligned}$$

which must be coupled with the manipulated Poisson equation for the spectral evolution (ongoing).

- **Dyson equation with external fields (only)** - VP system can be directly numerically integrated considering given mode evolution $|E_k(t)|$ extracted from simulation. Using $E_k = ik\varphi_k$:

$$\partial_\tau f_B = \partial_u \Gamma \ ,$$
$$\Gamma = \sum_j \ell_j^2 (\bar{\phi}_j \bar{G}_j^* + \bar{\phi}_j^* \bar{G}_j) \ ,$$
$$\partial_\tau \bar{G}_j = -i\ell_j u \bar{G}_j + \bar{\phi}_j \partial_u f_B \ ,$$

where $\bar{G}_j = e^{-i\ell_j u\tau} G_j$ and $G_j = \int_0^\tau dy e^{i\ell_j uy} \bar{\phi}_j \partial_u f_B$ (which corresponds to the normalized spectral components of the distribution function).

- Using tabulated $\bar{\phi}_j(\tau)$ from simulations, a Runge-Kutta ($4th$-order) evolves the system in time.

- Initial conditions: $f_B(0, u) =$(Gaussian-bump), and $\bar{G}_j(0, u) = 0$.

- Numerical results: **broad spectrum** (30 modes, Kubo no $\mathcal{K} \sim 0.03$).

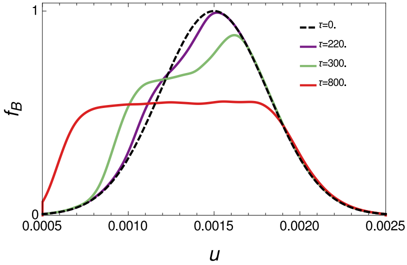

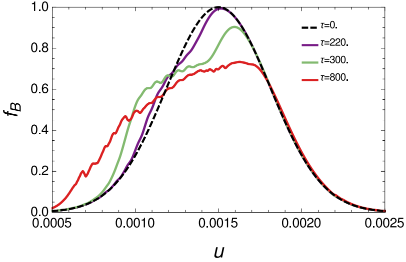

- (Very preliminary results).
- DysonExt seems less efficacious: mode-mode coopling(?)
- Numerical problem for integration (u-mesh) to be solved.

- **QL model** - Use the assumption of broad spectrum:

$$\sum_k (\ldots) \to \int_{k_{min}}^{k_{\max}} dk\, \mathcal{N}(k)(\ldots)\ ,$$

with the spectral density $\mathcal{N} = m/\Delta k$ ($\Delta k = \mathrm{Max}[k_j] - \mathrm{Min}[k_j]$).

- Fully consistent Dyson system can be manipulated to get:

$$\partial_t \hat{f}_B = \partial_t(\mathcal{D}\partial_v \hat{f}_B)\ , \qquad \mathcal{D} = (e^2\pi\mathcal{N}k^2/m^2)|\varphi|^2/v\ ,$$
$$\partial_t|\varphi|^2 = \pi\omega_p\eta v^2|\varphi|^2\partial_v \hat{f}_B\ .$$

- Using the dimensionless variables, this can be reduced to

$$f_B = F_B + \bar{\mathcal{N}} M\eta^{-1}\, \partial_u(\mathcal{J}u^{-5})\ ,$$
$$\partial_\tau \mathcal{J} = \pi\eta M^{-1}u^2\mathcal{J}\partial_u F_B + \pi\bar{\mathcal{N}}u^2\mathcal{J}\partial_u^2(\mathcal{J}u^{-5})\ ,$$

where $\mathcal{J}(\tau, u) = |\bar{\phi}|^2$, $\bar{\mathcal{N}} = m/\Delta\ell$ and $M = \int_{-\infty}^{+\infty} du F_B$.

- Spectral PDE integrated with (linearized) Crank-Nicolson algorithm.

- Numerical results: **broad spectrum** (30 modes, Kubo no $\mathcal{K} \sim 0.03$).

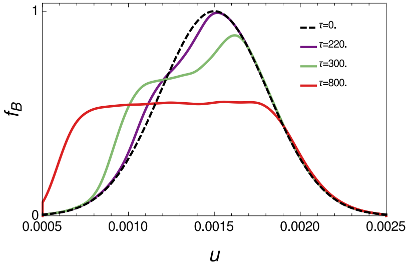

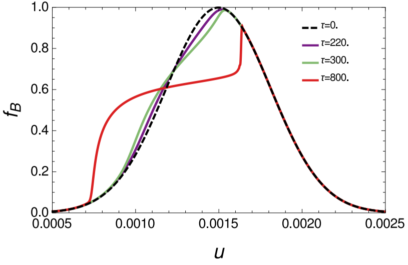

- QL less efficacious.
- Initial condition of QL contain $\partial_u \mathcal{J}$.
- QL results strongly depend on $\mathcal{J}(0, u)$ (linear phase).
- Implementation of a realistic spectral shape in the QL model.